

# nature

THE INTERNATIONAL WEEKLY JOURNAL OF SCIENCE

## EUROPA'S GREAT LAKES

*Watery origins for  
surface chaos on  
Jupiter's icy moon*

PAGES 482 & 502

### ARCHAEOLOGY

#### SPRING FEVER

*Planning a future  
for Egypt's past*

PAGE 464

### FOOD SECURITY

#### VANQUISHING FAMINE

*We have the technology — do  
we have the economics?*

PAGE 469

### PALAEOANTHROPOLOGY

#### EUROPEAN COMMUNITIES

*An early arrival for  
modern humans*

PAGES 484, 521 & 525

NATURE.COM/NATURE

24 November 2011 £10

Vol. 479, No. 7374





# Early dispersal of modern humans in Europe and implications for Neanderthal behaviour

Stefano Benazzi<sup>1</sup>, Katerina Douka<sup>2</sup>, Cinzia Fornai<sup>1</sup>, Catherine C. Bauer<sup>3</sup>, Ottmar Kullmer<sup>4</sup>, Jiří Svoboda<sup>5,6</sup>, Ildikó Pap<sup>7</sup>, Francesco Mallegni<sup>8</sup>, Priscilla Bayle<sup>9</sup>, Michael Coquerelle<sup>10</sup>, Silvana Condemi<sup>11</sup>, Annamaria Ronchitelli<sup>12</sup>, Katerina Harvati<sup>3,13</sup> & Gerhard W. Weber<sup>1</sup>

The appearance of anatomically modern humans in Europe and the nature of the transition from the Middle to Upper Palaeolithic are matters of intense debate. Most researchers accept that before the arrival of anatomically modern humans, Neanderthals had adopted several 'transitional' technocomplexes. Two of these, the Uluzzian of southern Europe and the Châtelperronian of western Europe, are key to current interpretations regarding the timing of arrival of anatomically modern humans in the region and their potential interaction with Neanderthal populations. They are also central to current debates regarding the cognitive abilities of Neanderthals and the reasons behind their extinction<sup>1–6</sup>. However, the actual fossil evidence associated with these assemblages is scant and fragmentary<sup>7–10</sup>, and recent work has questioned the attribution of the Châtelperronian to Neanderthals on the basis of taphonomic mixing and lithic analysis<sup>11,12</sup>. Here we reanalyse the deciduous molars from the Grotta del Cavallo (southern Italy), associated with the Uluzzian and originally classified as Neanderthal<sup>13,14</sup>. Using two independent morphometric methods based on microtomographic data, we show that the Cavallo specimens can be attributed to anatomically modern humans. The secure context of the teeth provides crucial evidence that the makers of the Uluzzian technocomplex

were therefore not Neanderthals. In addition, new chronometric data for the Uluzzian layers of Grotta del Cavallo obtained from associated shell beads and included within a Bayesian age model show that the teeth must date to ~45,000–43,000 calendar years before present. The Cavallo human remains are therefore the oldest known European anatomically modern humans, confirming a rapid dispersal of modern humans across the continent before the Aurignacian and the disappearance of Neanderthals.

Two deciduous molars (Cavallo-B and Cavallo-C) were excavated in 1964 from the site of Grotta del Cavallo (Apulia, southern Italy; Supplementary Information). Cavallo is important as the type site of the Uluzzian technocomplex<sup>15</sup>, one of the three main transitional industries alongside the Châtelperronian and Szeletian, in Franco-Cantabria and Central Europe, respectively. These are strongly suspected of being produced by Neanderthals, although the actual fossil evidence in association is scant<sup>16</sup>.

Cavallo-B is a deciduous left upper first molar (dM<sup>1</sup>), found in layer EIII (archaic Uluzzian). Cavallo-C is a deciduous left upper second molar (dM<sup>2</sup>) found 15–20 cm above Cavallo-B, in layer EII-I (evolved Uluzzian)<sup>13</sup> (Supplementary Fig. 1 and Supplementary Table 1). The specimens (Fig. 1) were described in 1967 by Palma di Cesnola and

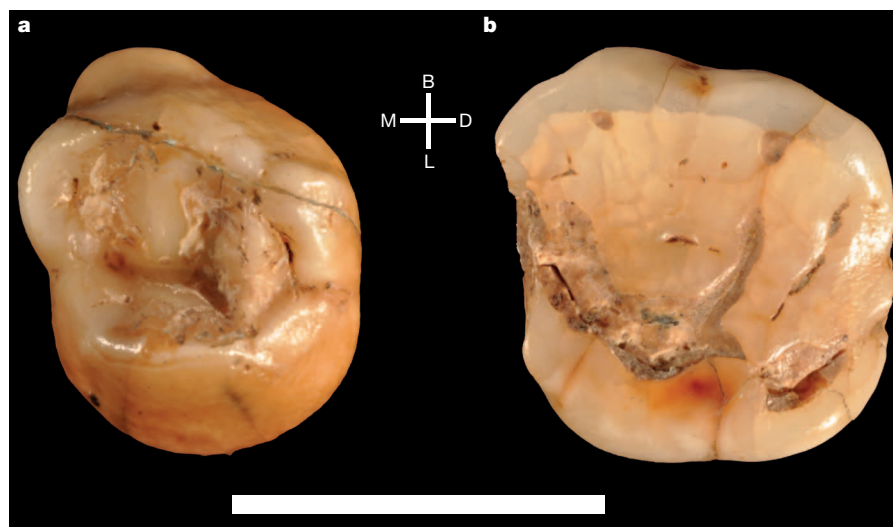


**Figure 1** | Occlusal view of the deciduous molars from the Uluzzian layers of Grotta del Cavallo (Apulia, southern Italy). **a**, Cavallo-B (deciduous left upper first molar; dM<sup>1</sup>). **b**, Cavallo-C (deciduous left upper second molar; dM<sup>2</sup>). B, buccal; D, distal; L, lingual; M, mesial. Scale bar, 1 cm.

<sup>1</sup>Department of Anthropology, University of Vienna, Althanstrasse 14, 1090 Vienna, Austria. <sup>2</sup>Oxford Radiocarbon Accelerator Unit, Research Laboratory for Archaeology and the History of Art, University of Oxford, Dyson Perrins Building, South Parks Road, Oxford OX1 3QY, UK. <sup>3</sup>Paleoanthropology, Department of Early Prehistory and Quaternary Ecology, Eberhard Karls Universität Tübingen, Rümelnstrasse 23, Tübingen 72070, Germany. <sup>4</sup>Department of Paleoanthropology and Messel Research, Senckenberg Research Institute Frankfurt, Senckenberganlage 25, D-60325 Frankfurt, Germany. <sup>5</sup>Institute of Archaeology, Academy of Sciences of the Czech Republic, Královopolská 147, 612 00 Brno, Czech Republic. <sup>6</sup>Department of Anthropology, Faculty of Science, Masaryk University, Viniřská 5, 603 00 Brno, Czech Republic. <sup>7</sup>Department of Anthropology, Hungarian Natural History Museum, Ludovika tér 2-6, 1083 Budapest, Hungary. <sup>8</sup>Department of Biology, University of Pisa, Via S. Maria 53, 56126 Pisa, Italy. <sup>9</sup>UMR 5199 PACEA, Université Bordeaux 1, avenue des Facultés, 33405 Talence, France. <sup>10</sup>Paleoanthropology group, Department of Paleobiology Museo Nacional de Ciencias Naturales (MNCN-CSIC), C/ José Gutiérrez Abascal 2, 28006 Madrid, Spain. <sup>11</sup>UMR 6578 CNRS/Aix Marseille/EFS, Laboratoire d'Anthropologie Bioculturelle, Faculté de Médecine/Secteur Nord, CS80011 Bd Pierre Dramard 13344, Marseille Cedex 15, France. <sup>12</sup>Department of Environmental Sciences "G. Sarfatti", U.R. Prehistoric Ecology, University of Siena, via T. Pendola 62, 53100 Siena, Italy. <sup>13</sup>Senckenberg Center for Human Evolution and Paleoecology, Eberhard Karls Universität Tübingen, Rümelnstrasse 23, Tübingen 72070, Germany.

Messeri<sup>13</sup> who classified Cavallo-B as modern human and Cavallo-C as Neanderthal. On this basis, the authors suggested a persistence of Neanderthal populations in southern Italy after the appearance of modern humans<sup>17</sup>.

Although information about these specimens is scarce and contradictory, most scholars accept that the deciduous molars from Grotta del Cavallo are attributable to Neanderthals, and therefore that Neanderthals produced the Uluzzian. This attribution was proposed by ref. 14 for Cavallo-B on the basis of the specimen's crown diameters (the dimensions of Cavallo-C were found to be compatible with both Neanderthals and anatomically modern humans). However, the Cavallo-B buccolingual and mesiodistal diameters used by ref. 14 appear to have been accidentally substituted for each other when compared to the crown diameters reported by ref. 13. The correct crown diameter values do not support Neanderthal affinities for Cavallo-B, neither does the crown morphology of the two specimens. Cavallo-B shows three dental cusps, typical of  $dm^1$  (ref. 10) from anatomically modern humans, with the lingual cusps mesially oriented and separated from the buccal cusps by a well-defined sagittal sulcus. Conversely, the  $dm^1$  of Neanderthals is more frequently four-cusped, with cusp tips compressed internally<sup>10</sup>. Cavallo-C has a sub-square crown outline, similar to  $dm^2$  of anatomically modern humans and different from the typical rhomboid outline with distolingual hypocone expansion of Neanderthal  $dm^2$ s (ref. 10).

To establish firmly the taxonomic affinities of the Cavallo human remains, we re-analysed Cavallo-B and Cavallo-C with two independent morphometric methods, using a comparative sample of Neanderthal, Upper Palaeolithic modern human (UPMH) and recent modern human (RMH)  $dm^1$  and  $dm^2$  specimens (Supplementary Tables 2–4).

Our first approach is a geometric morphometric analysis of outlines obtained from the dental crown<sup>18</sup> (see Methods), for which the group shape variation was evaluated through a shape-space principal component analysis (PCA).

For the  $dm^1$  crown outlines (Fig. 2a), the first two principal components (PCs) account for about 63% of the total variance. Neanderthals and modern humans separate along PC1 (42.7%), which characterizes size-independent shape variation ( $r = -0.33$ ;  $P = 0.06$ ). Neanderthal  $dm^1$  specimens show an ovoid outline, whereas RMH and UPMH specimens are more irregularly shaped for the presence of well-expressed tuberculum molare (molar tubercle of Zuckerkandl) and metacone (buccodistal) cusp, and for a general distolingual constriction due to the reduction of the hypocone. Cavallo-B plots well within the range of variability of the anatomically modern human sample. The cross-validation quadratic discriminant analysis (QDA) of the PC1 scores classified Cavallo-B as modern human with a posterior probability ( $P_{\text{post}}$ )  $> 0.90$  (Supplementary Table 4).

In the analysis of the  $dm^2$  cervical outlines (Fig. 2b), the first two PCs account for about 84% of the total variance. Neanderthals and anatomically modern humans are even more clearly separated along PC1 (71.4%), which expresses size-dependent shape variation (static allometry,  $r = 0.74$ ;  $P < 0.001$ ). Neanderthal  $dm^2$  specimens are characterized by a rhomboid cervical outline due to their large hypocone, whereas UPMH and RMH specimens have sub-square outlines. Cavallo-C plots unambiguously within the modern human range. The cross-validation QDA of the first two PC scores attributes Cavallo-C to modern human with a  $P_{\text{post}} > 0.90$  (Supplementary Table 4).

The second morphometric method considers the internal structure of the teeth and consists of the two-dimensional enamel thickness and dental tissue proportions analysis (Fig. 3) (see Methods and Supplementary Tables 3 and 4). The average and relative enamel thickness (AET and RET, respectively) have been described as effective taxonomic discriminators between Neanderthals and modern humans because Neanderthal molars are characterized by significantly thinner enamel relative to dentine volume<sup>19</sup>.

The  $dm^1$  modern human samples (UPMH and RMH) shown in Table 1 have been divided into sub-groups on the basis of their degree

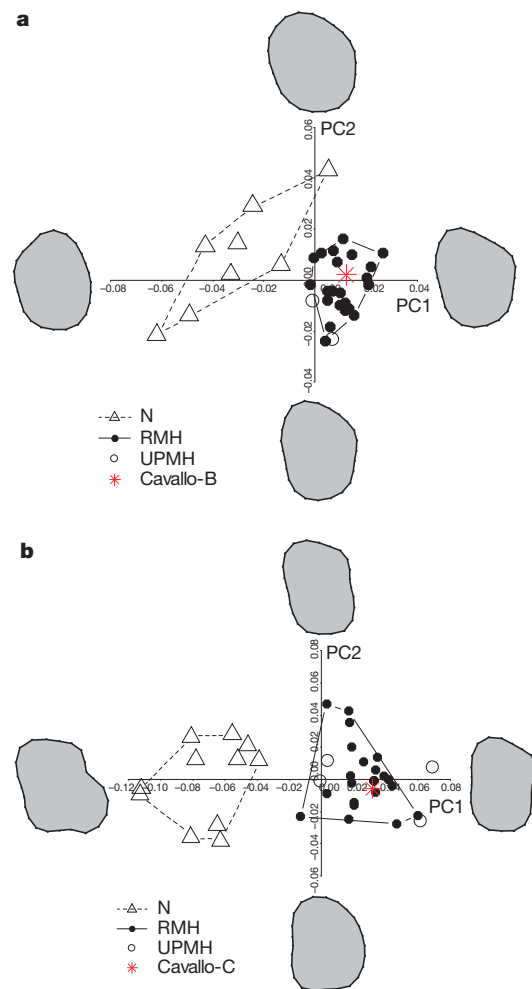


**Figure 2 | Shape-space PCA plots of  $dm^1$  crown outlines and  $dm^2$  cervical outlines. a,  $dm^1$  crown outline. b,  $dm^2$  cervical outline. The deformed mean crown outline in the direction of the PC is drawn at the extremity of each axis. N, Neanderthal; RMH, recent modern human; UPMH, Upper Palaeolithic modern human.**

of wear (unworn/wear stage 1 distinguished by wear stage 3; based on Smith<sup>20</sup>) to ease the comparison with the Neanderthal  $dm^1$  samples, which is entirely affected by wear stage 3. The Neanderthal  $dm^1$  RET indexes are significantly lower than those of RMH at similar wear stages ( $P < 0.001$ ; permutation test,  $n = 1,000$ ) on group mean and variance differences. The AET and RET indexes of Cavallo-B lie beyond the highest values computed so far for the unworn UPMH and RMH (Table 1). Considering that the RET index average difference from unworn to wear stage 3 for both RMH and UPMH is about 0.80, it is reasonable to assume that if Cavallo-B would have worn down to a wear stage 3, it would provide a RET index of approximately 11. This value is still completely outside the Neanderthal range of variation and near the highest values computed for the unworn RMH. The result further supports strongly the affiliation of Cavallo-B as anatomically modern human rather than Neanderthal.

With regard to the  $dm^2$  specimens (Table 1), the Neanderthal RET indexes are significantly lower than those of RMH ( $P < 0.001$ ). The UPMH specimens present the highest AET and RET indexes of the whole sample, RMH included. Cavallo-C is the most worn specimen within our  $dm^2$  sample (wear stage 5), therefore the AET and RET indexes result in a rather lower value than could be expected for the unworn stage of the same tooth. Nonetheless, both indexes still rank among the highest values obtained (Table 1). The cross-validation

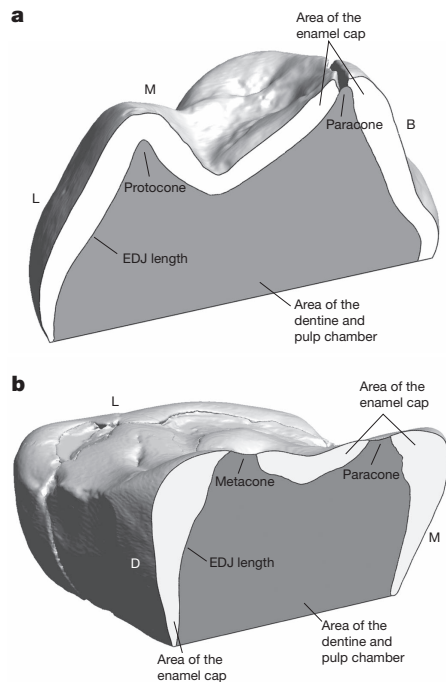


**Figure 3 | Cross-sections of Cavallo-B and Cavallo-C for two-dimensional enamel thickness analysis.** **a**, Buccolingual cross-section of Cavallo-B through the dentine horns of the protocone and paracone. **b**, Mesiodistal cross-section of Cavallo-C through the dentine horns of the paracone and metacone. B, buccal; D, distal; EDJ, enamel–dentin junction; L, lingual; M, mesial.

QDA of the  $dM^2$  RET index classifies Cavallo-C as modern human with a  $P_{\text{post}} > 0.90$  (Supplementary Table 4).

New radiocarbon dating of the Uluzzian layers was undertaken to produce a more robust chronology. Previous dates from the site disclosed inconsistency due to incomplete decontamination and unsuitability of the dated samples (Supplementary Information). In the absence of collagen from bone at the site and the lack of charcoal samples collected at the time of the excavation, marine shell samples were the only alternative and were therefore selected for dating. In the Uluzzian layers of Cavallo, several shells were transformed into beads, by snapping or piercing to produce personal ornaments. These beads are generally held to be an indicator of symbolic and complex behaviour. Eight shells of *Dentalium* sp., *Nuculana* sp. and *Cyclope neritea* were dated by accelerator mass spectrometry (AMS) radiocarbon dating following a novel methodological approach (Supplementary Information and Supplementary Fig. 3). The new dates were incorporated into a Bayesian model using the OxCal program (Supplementary Information) and calibrated against the INTCAL09 calibration curve<sup>21</sup> (Supplementary Figs 4 and 5 and Supplementary Tables 5 and 6). Layer EIII was calculated by the model to date between 45,010–43,380

(68.2% probability) and 47,530–43,000 (95.4% probability) calendar years before present (where present = 1950) (cal. yr BP). The distribution falls within Greenland Interstadial (GIS) 12, a long warm phase following Heinrich Event 5, and most likely towards its latter part. A decrease in temperature has been inferred based on the faunal assemblage from EIII (ref. 22). A likely initial arrival of anatomically modern humans during this post-HE5 interstadial has been suggested previously<sup>23</sup>. Layer EII-I, associated with a shell date of 40,000  $^{14}\text{C}$  yr BP, was modelled to date between 44,000–43,000 cal. yr BP (68.2% probability), a similar age to layer EIII. Comparable chronometric results were obtained from Grotta di Fumane, another Uluzzian site in the Italian pre-Alps and the only other with reliable chronometric information, where the technocomplex is dated at 44,800–43,900 cal. yr BP (95.4% probability) (or  $\sim 42,000$ –40,000  $^{14}\text{C}$  yr BP)<sup>24</sup>.

The new chronometric results show that the two deciduous molars from Grotta del Cavallo are the earliest European anatomically modern human fossils currently known. Because the Uluzzian technocomplex stratigraphically underlies the earliest Aurignacian in all instances where the two co-occur (for example, Grotta di Castelcivita, Grotta della Cala, Grotta La Fabbrica and Grotta di Fumane)<sup>5</sup>, the arrival of the earliest modern humans at these sites must pre-date the Aurignacian. Furthermore, considering that Neanderthals are likely to have survived in most of continental Europe until at least  $\sim 40,000$  cal. yr BP (ref. 25), our results offer fossil evidence for a longer period of co-existence in Europe between Neanderthals and modern humans.

The re-attribution of the teeth of Grotta del Cavallo to anatomically modern human has implications for the interpretation of the Uluzzian technocomplex<sup>14,16</sup>. The presence of personal ornaments in the form of marine shell beads, worked bone and colorants—including ochre and limonites—in the Uluzzian layers of Grotta del Cavallo<sup>5,6</sup> has been used as direct evidence for Neanderthals reaching behavioural modernity independent of, and before, anatomically modern humans reaching Europe<sup>1,26</sup>. These attributes are all more typical of Upper Palaeolithic industries. This multiple species model for the origin of fully modern behaviour has been considered by some to be an impossible coincidence<sup>27</sup> and a fervent debate has ensued among prehistorians on the behavioural and cognitive capabilities of the makers of the transitional industries found across Europe and the Levant. Our results show that the Uluzzian is not a Neanderthal industry.

Stratigraphically, the Uluzzian is always separated from the final Mousterian by sterile layers, volcanic ash (as in Cavallo), erosional discontinuities or depositional hiatuses, which might suggest that a period of time has elapsed between the two phases. In southern Italy, economic and cultural behaviour of the Uluzzian suggests a greater affinity with the succeeding Aurignacian (with marginally backed tools) than with the final Mousterian<sup>5,6,22</sup>. These findings provide additional support for a modern human authorship of the Uluzzian. Although we cannot extrapolate our conclusions to other transitional industries, our findings indicate that caution should be applied when associating Neanderthals with them, particularly the Châtelperronian and Szeletian (see details of the ongoing debate on this topic<sup>2–4,9,11,12</sup>).

**Table 1 | Two-dimensional enamel thickness of Cavallo-B and Cavallo-C compared with the indicated  $dM^1$  and  $dM^2$  samples.**

Tooth	Taxon	Wear stage*	n	AET (mm)		RET (scale free)	
				Mean	Range	Mean	Range
$dM^1$	Neanderthal	3	6	0.40 (0.03)	0.37–0.45	7.17 (0.54)	6.61–7.93
$dM^1$	UPMH	3	2	0.51 (0.01)	0.50–0.52	9.56 (0.13)	9.47–9.66
$dM^1$	RMH	3	14	0.47 (0.03)	0.43–0.52	9.12 (0.67)	8.50–10.52
$dM^1$	UPMH	Unworn	1	0.56	–	10.36	–
$dM^1$	RMH	Unworn–stage 1	8	0.51 (0.06)	0.41–0.58	9.96 (0.96)	8.66–11.36
$dM^1$	Cavallo-B	Unworn	1	0.69	–	11.80	–
$dM^2$	Neanderthal	Unworn–stage 1	9	0.63 (0.04)	0.58–0.69	10.89 (0.84)	9.60–12.39
$dM^2$	UPMH	Stage 1–stage 2	2	0.97 (0.15)	0.86–1.07	17.93 (1.40)	16.94–18.92
$dM^2$	RMH	Unworn–stage 3	23	0.73 (0.08)	0.56–0.93	13.84 (1.53)	11.43–18.00
$dM^2$	Cavallo-C	Stage 5	1	0.84	–	14.28	–

Standard deviation is indicated in brackets. AET, average enamel thickness index; RET, relative enamel thickness index; RMH, recent modern human; UPMH, Upper Palaeolithic modern human.

\*Based on ref. 20.



The association of the Uluzzian with anatomically modern humans implies much greater complexity and age depth to the movement of modern humans into Europe and may lend support to a southern Mediterranean route in their dispersal, similar to that identified previously<sup>27</sup> for the spread of the Aurignacian. Although it is during the Aurignacian that certain technological and behavioural innovations effloresce, such as blade and bladelet-dominated lithic assemblages, bone and ivory tools, art and personal ornaments, the initial appearance of these traits in southern Europe clearly pre-dates this. This discovery has significant implications for our understanding of the earliest presence of anatomically modern humans in Europe, expands the period of overlap between modern humans and Neanderthals and makes it much less likely that Neanderthals developed their own Upper Palaeolithic suite of behaviours before the arrival of anatomically modern humans.

## METHODS SUMMARY

The comparative dental sample for both the morphometric outline analyses and the two-dimensional enamel thickness and dental tissue proportions analysis is provided in Supplementary Table 2.

Scans of all the specimens were undertaken by means of industrial and synchrotron-based microtomographic scanners at isotropic voxel length between 15 and 55 µm. The microtomographic image stacks of each tooth were aligned with the cervical plane parallel to the *x-y* plane of the Cartesian coordinate system. The three-dimensional digital surface models were created semi-automatically by threshold-based segmentation, contour extraction and surface reconstruction.

For the outline analyses we considered the dM<sup>1</sup> crown outlines because Cavallo-B is unworn; conversely, we used the cervical outlines of the dM<sup>2</sup> samples, as Cavallo-C shows both occlusal and interproximal wear. To identify the crown outline and the cervical outline we followed the procedures described previously<sup>18</sup>, with some adjustment for our specific case.

For the analyses of the two-dimensional enamel thickness and dental tissue proportions, the following measurements were recorded: the area of the enamel cap (mm<sup>2</sup>), the area of the coronal dentine (which includes the coronal pulp; mm<sup>2</sup>), the length of the enamel–dentine junction (EDJ; mm), the average enamel thickness (AET) index (the area of the enamel cap divided by the length of the EDJ; index in mm) and the RET index (the average enamel thickness divided by the square root of the coronal dentine area; scale free index)<sup>19,28</sup>. The data were analysed via software routines written in R<sup>29</sup> (Supplementary Information).

**Full Methods** and any associated references are available in the online version of the paper at [www.nature.com/nature](http://www.nature.com/nature).

Received 30 August; accepted 5 October 2011.

Published online 2 November 2011.

1. d'Errico, F., Zilhão, J., Julien, M., Baffier, D. & Pélegrin, J. Neanderthal acculturation in Western Europe? A critical review of the evidence and its interpretation. *Curr. Anthropol.* **39**, 1–44 (1998).
2. Gravina, B., Mellars, P. & Ramsey, C. B. Radiocarbon dating of interstratified Neanderthal and early modern human occupations at the Châtelperronian type-site. *Nature* **438**, 51–56 (2005).
3. Mellars, P., Gravina, B. & Bronk Ramsey, C. Confirmation of Neanderthal/modern human interstratification at the Châtelperronian type-site. *Proc. Natl Acad. Sci. USA* **104**, 3657–3662 (2006).
4. Zilhão, J. *et al.* Analysis of Aurignacian interstratification at the Châtelperronian-type site and implications for the behavioral modernity of Neandertals. *Proc. Natl Acad. Sci. USA* **103**, 12643–12648 (2006).
5. Ronchitelli, A., Boscolo, P. & Gambassini, P. in *La lunga storia di Neandertal. Biologia e comportamento* (eds Facchini, F. & Belcastro, G. M.) (Jaca Book, 2009).
6. d'Errico, F., Borgia, V. & Ronchitelli, A. Uluzzian bone technology and its implications for the origin of behavioural modernity. *Quat. Int.* doi:10.1016/j.quaint.2011.03.039 (in the press).
7. Lévêque, F. & Vandermeersch, B. M. Découverte de restes humains dans un niveau castelperronien à Saint-Césaire (Charente-Maritime). *CR Acad. Sci. Paris* **291**, 187–189 (1980).
8. Hublin, J. J., Spoor, F., Braun, M., Zonneveld, F. & Condemi, S. A late Neanderthal associated with Upper Palaeolithic artefacts. *Nature* **381**, 224–226 (1996).
9. Harvati, K., Panagopoulou, E. & Karkanas, P. First Neanderthal remains from Greece: the evidence from Lakonis. *J. Hum. Evol.* **45**, 465–473 (2003).
10. Bailey, S. E. & Hublin, J. J. Dental remains from the Grotte du Renne at Arcy-sur-Cure (Yonne). *J. Hum. Evol.* **50**, 485–508 (2006).
11. Bar-Yosef, O. & Bordes, J. G. Who were the makers of the Châtelperronian culture? *J. Hum. Evol.* **59**, 586–593 (2010).

12. Higham, T. *et al.* Chronology of the Grotte du Renne (France) and implications for the context of ornaments and human remains within the Châtelperronian. *Proc. Natl Acad. Sci. USA* **107**, 20234–20239 (2010).
13. Palma di Cesnola, A. & Messeri, M. P. Quatre dents humaines paléolithiques trouvées dans des cavernes de l'Italie Méridionale. *L'Anthropologie* **71**, 249–262 (1967).
14. Churchill, S. E. & Smith, F. H. Makers of the early Aurignacian of Europe. *Am. J. Phys. Anthropol.* **113** (Suppl. 31), 61–115 (2000).
15. Palma di Cesnola, A. L'Uluzzien: faciès italien du leptolithique archaïque. *L'Anthropologie* **93**, 783–812 (1989).
16. Riel-Salvatore, J. in *Sourcebook of Paleolithic Transitions* (eds Camps, M. & Chauhan, P.) (Springer, 2009).
17. Messeri, P. & Palma di Cesnola, A. Contemporaneità di paleantropi e fanerantropi sulle coste dell'Italia meridionale. *Zephyrus* **26–27**, 7–30 (1976).
18. Benazzi, S. *et al.* Comparison of dental measurement systems for taxonomic assignment of first molars. *Am. J. Phys. Anthropol.* **144**, 342–354 (2011).
19. Olejniczak, A. J. *et al.* Dental tissue proportions and enamel thickness in Neandertal and modern human molars. *J. Hum. Evol.* **55**, 12–23 (2008).
20. Smith, B. H. Patterns of molar wear in hunter-gatherers and agriculturists. *Am. J. Phys. Anthropol.* **63**, 39–56 (1984).
21. Reimer, P. J. *et al.* IntCal09 and Marine09 radiocarbon age calibration curves, 0–50,000 years cal BP. *Radiocarbon* **51**, 1111–1150 (2009).
22. Boscolo, P. & Crezzini, J. Middle-Upper Palaeolithic transition in Southern Italy: Uluzzian macromammals from Grotta del Cavallo (Apulia). *Quat. Int.* doi:10.1016/j.quaint.2011.03.028 (in the press).
23. Müller, U. C. *et al.* The role of climate in the spread of modern humans into Europe. *Quat. Sci. Rev.* **30**, 273–279 (2011).
24. Higham, T. European Middle and Upper Palaeolithic radiocarbon dates are often older than they look: problems with previous dates and some remedies. *Antiquity* **85**, 235–249 (2011).
25. Pinhasi, R., Higham, T. F., Golovanova, L. V. & Doronichev, V. B. Revised age of late Neanderthal occupation and the end of the Middle Paleolithic in the northern Caucasus. *Proc. Natl Acad. Sci. USA* **108**, 8611–8616 (2011).
26. Zilhão, J. in *Continuity and Discontinuity in the Peopling of Europe* (eds Condemi, S. & Weniger, G. C.) (Springer, 2011).
27. Mellars, P. The impossible coincidence: a single species model for the origins of modern human behavior in Europe. *Evol. Anthropol.* **14**, 12–27 (2005).
28. Martin, L. B. Significance of enamel thickness in hominoid evolution. *Nature* **314**, 260–263 (1985).
29. R Development Core Team. R: a language and environment for statistical computing. (<http://www.r-project.org>) (2008).

**Supplementary Information** is linked to the online version of the paper at [www.nature.com/nature](http://www.nature.com/nature).

**Acknowledgements** We thank the Soprintendenza per i Beni Archeologici della Puglia which facilitated the excavation of Grotta del Cavallo over the years. We also thank M. A. Gorgoglione who supported and helped in the collection of samples for <sup>14</sup>C dating and encouraged the collaboration with the University of Siena for the study of the archaeological remains. P. Boscolo, H. Klempererova, F. Ranaldo and S. Ricci have all helped in aspects of the research and are especially thanked. We are grateful to G. Gruppioni for providing the Italian modern human sample used in this work. We thank M. Francken, B. Trautmann, I. Trautmann, H. Scherf, M. Dockner and R. Ginner for technical assistance. We thank F. L. Bookstein for suggestions on statistics. Access to the fossil specimens was made possible by the Croatian National History Museum, the French Musée National de Préhistoire, the French Muséum National d'Histoire Naturelle, Paleoanthropology, Eberhard Karls Universität Tübingen and the NESPOS Database 2011 (<https://www.nespos.org/display/openspace/Home>). We acknowledge the Centre de Microtomographie (Université de Poitiers), the Vienna micro-CT Laboratory (University of Vienna), VISCOM AG Hannover, the Paleoanthropology High Resolution Computing Tomography Laboratory (Eberhard Karls Universität Tübingen), the European Synchrotron Radiation Facility beamline ID17, the AST-RX platform (French Muséum National d'Histoire Naturelle) and the Oxford Radiocarbon Accelerator Unit (ORAU). The authors would like to thank T. Higham and R. E. M. Hedges for their input in the radiocarbon dating part of the project, for important comments and proofreading this manuscript. The radiocarbon dating was funded by the Natural Environment Research Council (NERC) NRCF programme. K.D. is part of the Ancient Human Occupation of Britain project, funded by the Leverhulme Trust. This work was supported by the NSF 01-120 Hominid Grant 2007, A.E.R.S. Dental Medicine Organisations GmbH FA547013, the Fondation Fyssen, the DFG INST 37/706-1 FUGG and the NERC Grant (NE/D014077/1).

**Author Contributions** S.B., F.M., K.H. and G.W.W. initiated and organized the project. S.B., C.C.B., P.B., J.S., I.P., K.H. and G.W.W. collected the fossils and modern human sample. S.B. and C.F. carried out the dental measurements. S.B. and M.C. analysed the data. K.D. initiated and performed the radiocarbon dating project. S.B., K.D., C.F., O.K., M.C., S.C., A.R., K.H. and G.W.W. discussed the results. S.B., K.D., C.F., M.C., S.C., A.R., K.H. and G.W.W. wrote and edited the manuscript.

**Author Information** Reprints and permissions information is available at [www.nature.com/reprints](http://www.nature.com/reprints). The authors declare no competing financial interests. Readers are welcome to comment on the online version of this article at [www.nature.com/nature](http://www.nature.com/nature). Correspondence and requests for materials should be addressed to S.B. ([stefano.benazzi@univie.ac.at](mailto:stefano.benazzi@univie.ac.at)).

## METHODS

### Scanning, segmentation and three-dimensional reconstruction of the specimens.

Microtomographic scans of all the specimens (Supplementary Table 2) were undertaken by means of industrial and synchrotron-based microtomographic scanners at isotropic voxel length between 15 and 55  $\mu\text{m}$ . The microtomographic image stacks of each tooth were aligned to the best-fit plane computed at the cervical line (cervical plane) through Amira 5.3 (Mercury Computer Systems), and then rotated up so that the cervical plane was parallel to the  $x$ - $y$  plane of the Cartesian coordinate system. For the segmentation process, the half-maximum height (HMH) protocol was used to reconstruct three-dimensional digital surface models of each microtomography-scanned tooth using Amira 5.3 (Supplementary Information).

**Outline data.** A further orientation of the  $\text{dM}^1$  and  $\text{dM}^2$  digital models in the Cartesian coordinate system was required before the outline analysis. The  $\text{dM}^1$  oriented digital models were rotated around the  $z$  axis to align the projection on the  $x$ - $y$  plane of the intercept between the paracone and protocone cusp tips parallel to the  $y$  axis of the Cartesian coordinate system. The crown outlines were then projected onto the  $x$ - $y$  plane. The  $\text{dM}^2$  digital models were oriented with the lingual side parallel to the  $x$  axis. The best-fit plane of the cervical line identified the cervical outline. In one case (the Neanderthal specimen Engis 2), computer-aided design (CAD) techniques were used to restore the  $\text{dM}^1$  crown outline (Supplementary Fig. 2).

All the outlines were represented by 24 landmarks obtained by equiangularly spaced radial vectors out of the centroid of their area<sup>18</sup>. These landmarks were superimposed through a generalized Procrustes analysis (GPA)<sup>30</sup>. Since the outlines were oriented and centred on the centroid of their area<sup>18</sup>, GPA only entailed a uniform scaling of the landmark configurations to unit centroid size. This step removed size differences, except for static allometry.

**Two-dimensional enamel thickness data.** For the two-dimensional enamel thickness assessment we followed techniques developed previously<sup>28</sup>, adapted to our specific case. A plane perpendicular to the cervical plane of the tooth and passing through two dentine horn tips was used for sectioning the dental crowns. The section passed through the  $\text{dM}^1$ 's paracone and protocone dentine horn tips, and through the  $\text{dM}^2$ 's paracone and metacone dentine horn tips (Fig. 3). The dentine horn tips were identified as the highest points of the dentine in the central mammelon by scrolling apically through the oriented slices. For Cavallo-C (wear stage 5; based on Smith<sup>20</sup>) and the comparative sample with wear stage 3, this approach was further verified by segmenting the whole crown dentine to check the continuity of the marginal ridges beside the dentine horns. For worn teeth, the EDJ length was truncated at the exposed edge of the occlusal dentine basins.

Cavallo-B shows a crack crossing the paracone mesiodistally (Fig. 3a). The area of the crack pertaining to the dentine was included in the dentine area, and the trait

of the EDJ intersected by the crack was calculated in the EDJ length. On the contrary, the missing area of the enamel cap was not reconstructed. Therefore, the computed RET index for Cavallo-B is slightly underestimated.

The segmentation process and the parameter measurements were carried out by S.B. and C.F. The interobserver error was evaluated for the enamel and dentine area of three of the fossil specimens from our sample, and did not exceed 3% in each case.

The following measurements were recorded: the area of the enamel cap ( $\text{mm}^2$ ), the area of the coronal dentine (which includes the coronal pulp;  $\text{mm}^2$ ), the length of the enamel-dentine junction (EDJ; mm), the average enamel thickness (AET) index (the area of the enamel cap divided by the length of the EDJ; index in mm) and the RET index (the average enamel thickness divided by the square root of the coronal dentine area; scale free index)<sup>19,28</sup>.

**Statistical analysis.** A Principal component analysis (PCA) of the matrix of Procrustes coordinates was carried out for the  $\text{dM}^1$  crown outlines and  $\text{dM}^2$  cervical outlines, separately. Because we aimed at assessing the dental outline shapes of the teeth from Grotta del Cavallo with respect to both the anatomically modern human and the Neanderthal outline shape variation, Cavallo-B and Cavallo-C spatial configurations were projected into the space built from the comparative sample only. In the Supplementary Information we show that the first PC of  $\text{dM}^1$  crown outlines PCA and the first two PCs of  $\text{dM}^2$  cervical outlines PCA are the only informative ones.

We did not regress the part of radial size correlated with the diameters, diagonals and area out of the crown and cervical outline data (as previously suggested<sup>18</sup> for the first permanent molars) because size information related to static allometry is an important factor for the separation of Neanderthal and anatomically modern human  $\text{dM}^2$ s.

The differences between the AET and RET indexes of Neanderthal and RMH were tested via a permutation test ( $n = 1,000$ ) on group mean and variance.

Finally, we used leave-one-out cross-validation quadratic discriminant analysis (QDA) for the taxonomic classification of Cavallo-B and Cavallo-C. We built up QDA models leaving out the data from the Cavallo specimens. The computation of the posterior probabilities ( $P_{\text{post}}$ ) was made with an equal prior probability ( $P_{\text{prior}}$ ) of 0.5 for Neanderthal and anatomically modern human groups (UPMH plus RMH). The threshold for taxonomic determination was a  $P_{\text{post}} \geq 0.90$ . The taxonomic analyses are summarized in the Supplementary Information. The data were processed and analysed through software routines written in R<sup>29</sup>.

30. Rohlf, F. J. & Slice, D. E. Extensions of the Procrustes method for the optimal superimposition of landmarks. *Syst. Zool.* **39**, 40–59 (1990).